JOURNAL OF GEOPHYSICAL RESEARCH, VOL. 102, NO. A9, PAGES 19,773–19,778, SEPTEMBER 1, 1997

Shadowed particle distributions near the Moon

S. D. Bale[1]

Astronomy Unit, Queen Mary and Westfield College, London, England

Abstract. Recent Wind spacecraft observations of broadband ion acoustic noise and Langmuir waves near the lunar wake suggest that the electron dynamics play an important role in the solar wind-Moon interaction. As the solar wind flows past the Moon, electrons and ions impacting the lunar surface are removed from their respective distribution functions. We extend a guiding center model of the solar wind velocity distribution into two dimensions and include separate electron and ion distributions. While the ion density shadow is predominantly in the antisunward direction, the electrons have density shadows that extend roughly along the direction of the interplanetary magnetic field lines tangent to the Moon. The charge imbalance created by the topological difference of these density distributions must induce space charge fields in the solar wind plasma; these may drive currents that generate the observed ion acoustic noise. Unstable positive slope features in the electron distribution function arise naturally in this scenario. Langmuir waves would then be generated by a time-of-flight cutoff distribution as in the terrestrial electron foreshock. This model is not self-consistent, as it does not include space charge effects, but serves to point out the importance of considering a kinetic description of the solar wind-Moon interaction.

1. Introduction

During a lunar flyby manuever in December 1994, the Wind spacecraft observed ion acoustic, Langmuir, and whistler waves [*Kellogg et al.*, 1996; *Farrell et al.*, 1996; *Bale et al.*, 1997] in the vicinity of the Moon; several subsequent encounters show similar wave activity. It has recently been shown that these observations occur when the spacecraft is magnetically connected to the Moon/wake system and further that a simple guiding center model may explain the observations [*Bale et al.*, 1997]. During the December 1994 flyby, ion acoustic waves were observed at 8 R_m upstream and downstream from the lunar wake and Langmuir waves and beam modes were observed as Wind approached the magnetic field lines tangent to the Moon. Other close lunar approaches have shown ion acoustic noise and Langmuir waves on connected field lines at distances greater than 40 R_m from the Moon (e.g., around 2000 UT on August 17, 1996). The Explorer 35 spacecraft observed regions of depleted electron density near the Moon [*Lin*, 1968; *Van Allen and Ness*, 1969] and found them to be correlated with the direction of the interplanetary magnetic field (IMF). A related observation was made by *Weber et al.* [1976], who observed wave activity with the RAE-2 spacecraft at 25-110 kHz near the Moon. These frequencies are in the range of the solar wind electron plasma frequency and imply some effect on the local electron distribution function.

Whang [1968] used a guiding center model of the solar wind proton population to explain Explorer 35 observations of an ion density depletion antisunward of the Moon. In this model, it was assumed that the electrons, with a higher thermal speed, were bound to the ions and would fill in the wake accordingly. Since both the ion and electron Larmor radii are much smaller than the lunar disc and the Moon's intrinsic magnetic moment is essentially zero [*Schubert and Lichtenstein*, 1974], any solar wind particles incident on the lunar surface are absorbed and removed from their respective velocity distribution functions. There is therefore no lunar bow shock or associated suprathermal particle flux. Indeed, the solar wind spectrometer experiment on Apollo 15 observed comparable solar wind electron and proton densities at the lunar surface [*Goldstein*, 1974].

If one assumes that all particles on straight-line paths that intersect the Moon are removed from the solar wind, then the velocity-space relationship $\gamma_{\|} \sin(\beta-\phi)+\gamma_{\perp}\cos(\beta-\phi)=\sin\beta$ can be derived where $\beta=\lambda\mp\alpha$, $\alpha=\sin^{-1}(\sqrt{1-Z_{sc}^2}/\sqrt{X_{sc}^2+Y_{sc}^2})$, $\lambda=\tan^{-1}(Y_{sc}/X_{sc})$ and $\phi=\tan^{-1}(B_y/B_x)$ in a right-handed frame with no $\hat{Z}$ component of the IMF and $\hat{X}$ in the solar wind flow direction. This gives two values each of $\gamma_{\|}=v_{\|}/v_{sw}$ and $\gamma_{\perp}=v_{\perp}/v_{sw}$, corresponding to $\beta=\lambda-\alpha$ and $\beta=\lambda+\alpha$, within which the solar wind distributions are removed.

[1]Now at Space Sciences Laboratory, University of California, Berkeley.

Paper number 97JA01676.
0148-0227/97/97JA-01676$09.00

Writing the particle velocity as $\vec{v} = v \cos\delta \hat{\|} + v \sin\delta \hat{\perp}$, the two cutoff parameters can be written

$$\gamma_1 = \frac{v_1}{v_{sw}} = \frac{\sin(\alpha+\lambda)}{\sin(\phi-\alpha-\lambda-\delta)} \quad (1a)$$

$$\gamma_2 = \frac{v_2}{v_{sw}} = \frac{\sin(\alpha-\lambda)}{\sin(\phi+\alpha-\lambda-\delta)} \quad (1b)$$

where δ is the particle pitch angle. If one assumes that the solar wind distributions, in the flow frame, are Maxwellian parallel to the IMF and have only Larmor motion in the perpendicular directions (guiding center approximation) then $\delta = 0$ in (1) above and (3) of [*Whang*, 1968] is recovered. We will proceed with $\delta = 0$ but would point out that the pitch angle dependence of the velocity cutoff implies that the guiding center model is not strictly true. In particular, the form of $\gamma(\delta)$ is such that γ_1 and γ_2 define two nonparallel lines in velocity space within which the solar wind particles are absent; where these lines cross $v_\perp = 0$, we have the guiding center solution. The growth of electrostatic Langmuir waves depends chiefly on features in the parallel, or reduced, velocity distribution; however, this anisotropy of the shadowing has implications for the generation of electromagnetic wave modes.

Whang [1968] defines three disturbed regions of solar wind; in the disturbed regions, the parallel particle distribution is Maxwellian in the intervals $(-\infty, -\gamma_1 v_{sw})$ in region I, $(\gamma_2 v_{sw}, \infty)$ in region II, and $(-\infty, -\gamma_1 v_{sw}) \cup (\gamma_2 v_{sw}, \infty)$ in region III. These regions, with the above angles, are shown in Figure 1. Figure 1 also shows a schematic of the shadowed electron distribution functions. The gaps in the distribution result in a depleted density region.

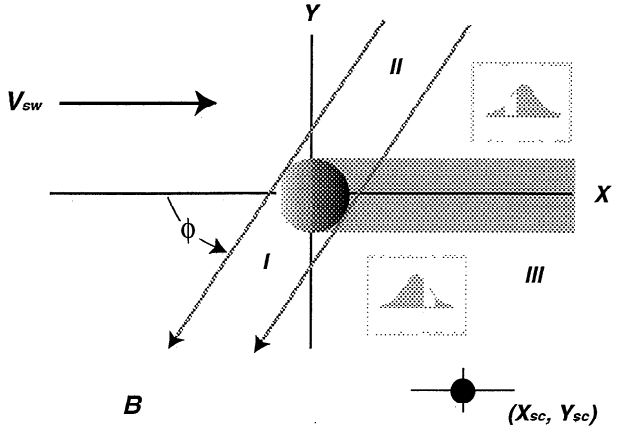

Figure 1. The geometry of the model. The $\hat{X}$ axis points along the solar wind flow direction and the IMF vector lies in the $\hat{X}$-$\hat{Y}$ plane. The regions I, II, and III are characterized by shadowed particle distributions and are described in the text. Schematic guiding center particle distributions are shown in the inset boxes; these distributions have inherently unstable features.

2. Density Depletions

Using the particle velocity distributions Maxwellian in the intervals given above, the species density can be calculated as

$$\left.\frac{n_s}{n_0}\right|_I = \frac{1}{2}\,\mathrm{erfc}(\gamma_1 S_s) \quad (2a)$$

$$\left.\frac{n_s}{n_0}\right|_{II} = \frac{1}{2}\,\mathrm{erfc}(\gamma_2 S_s) \quad (2b)$$

$$\left.\frac{n_s}{n_0}\right|_{III} = \frac{1}{2}\left(\mathrm{erfc}(\gamma_1 S_s) + \mathrm{erfc}(\gamma_2 S_s)\right) \quad (2c)$$

where erfc(x) is the complementary error function of x, $S_s = v_{sw}/v_{th}^s$ and γ_1 and γ_2 are as above; the subscripts I, II, and III refer to the regions defined in section 1. We use speed ratios of $S_i = 10$ and $S_e = 10/43$ and a field angle $\phi = \pi/4$ which are consistent with the solar wind parameters during the December 1994 Wind lunar encounter [*Ogilvie et al.*, 1996; *Bosqued et al.*, 1996; *Owen et al.*, 1996]. Likewise, the particle flux can be evaluated in closed form by integrating for the first moment of the disturbed distribution function. Figure 2 shows the spatial distribution of the ion density (Figure 2a) and the electron density (Figure 2b) as calculated from (2). The ion density distributions are essentially the same as those reported by *Whang* [1968]. It can be seen that in addition to the antisunward ion wake, the regions along and just behind the tangent IMF lines to the Moon are depleted of electrons. As λ approaches the angles $\phi \pm \alpha$, the two cutoff parameters (equation 1) approach infinity. The competition between the increasingly larger velocity gap (and hence more shadowed electrons) and the decaying tail of the electron distribution function forces the electron density minima to lie just antisunward of the tangent IMF lines to the Moon. This is presumably the observation made by *Lin* [1968], who found density depletions near the tangent IMF lines. As S is increased, by higher solar wind speed or lower electron temperature, these electron depletion wings will be forced back toward the antisunward region.

3. Unstable Velocity Distributions

Figure 1 schematically shows the form of the distribution functions in region III. Since the electron velocity distribution has a gap in this region, there must be a positive slope feature in the distribution function. It is well accepted that a similar "cutoff" distribution function is responsible for the intense Langmuir wave activity near the solar wind-electron foreshock boundary [*Filbert and Kellogg*, 1979; *Cairns*, 1987]. Wind observed Langmuir waves and beam modes as the spacecraft approached the tangent magnetic field line to the Moon on December 27, 1994. Such waves would be gen-

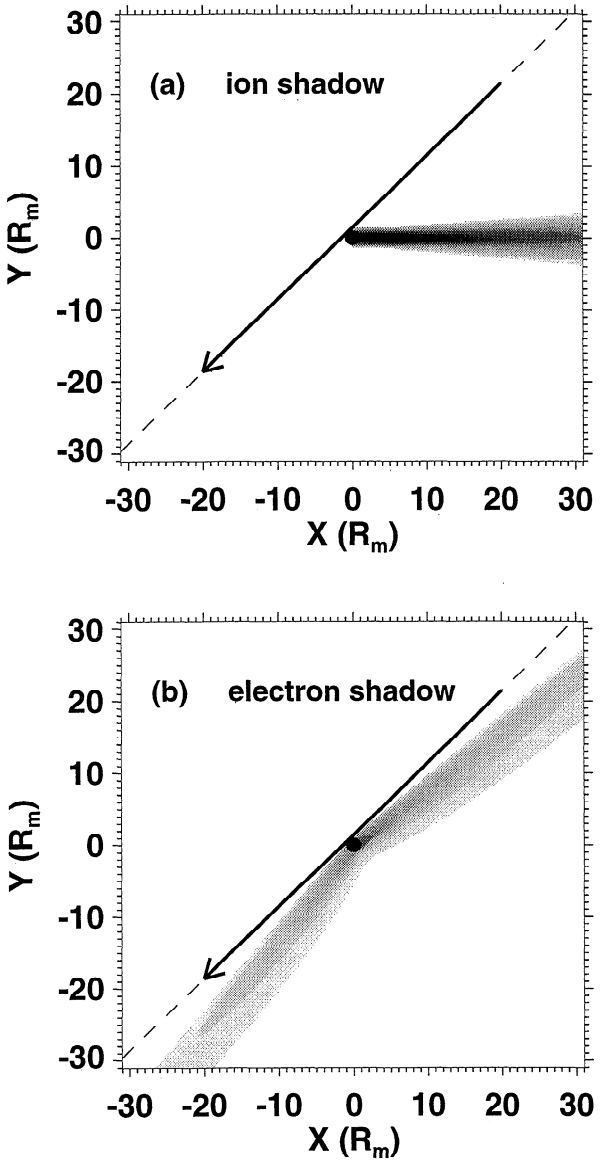

Figure 2. The ion and electron density shadows for $S_i = 10$ and $S_e = 10/43$. (a) The region of depleted proton density due to lunar shadowing; the arrow is along the direction of the IMF. This is the result obtained by *Whang* [1968]. (b) The region of electron density depletion. The electron density shadow is guided by, and swept back from, the IMF direction. Since these regions contain a nonneutral plasma, space charge fields will arise to enforce neutrality.

erated by the positive slope features in the shadowed electron distribution. Indeed, the beam mode waves were observed farther from the tangent lines where the velocity cutoff is closer to the electron thermal speed; this would be expected if the physics is analogous to that of the terrestrial electron foreshock. *Weber et al.* [1976] observed similar wave activity near the plasma frequency on the RAE-2 satellite and concluded that it was related to the disturbed electron distributions near the Moon. Preliminary data analysis shows that the amplitude of the Langmuir waves falls off with distance from the tangent line, as is the case with the solar wind-terrestrial electron foreshock boundary.

4. A Mass Spectrometer

The parameter controlling the shape of the density wake in (2) is $S_s = v_{sw}/v_{th}^s$; when S is large, the wake is antisunward and controlled by the flow direction of the solar wind. Small values of S result in a wake whose direction is controlled by the IMF angle. Figure 3 shows the shape of the ion and electron shadows for values $S_i = 1$ and $S_e = 1/43$; this corresponds to $v_{sw} = v_{th}^p$, which is unrealistic in the solar wind but serves to show the dependence of the density shadows on S. In this regime, the ion shadow has begun to recede toward the tangent IMF lines, and the electron density shadow is

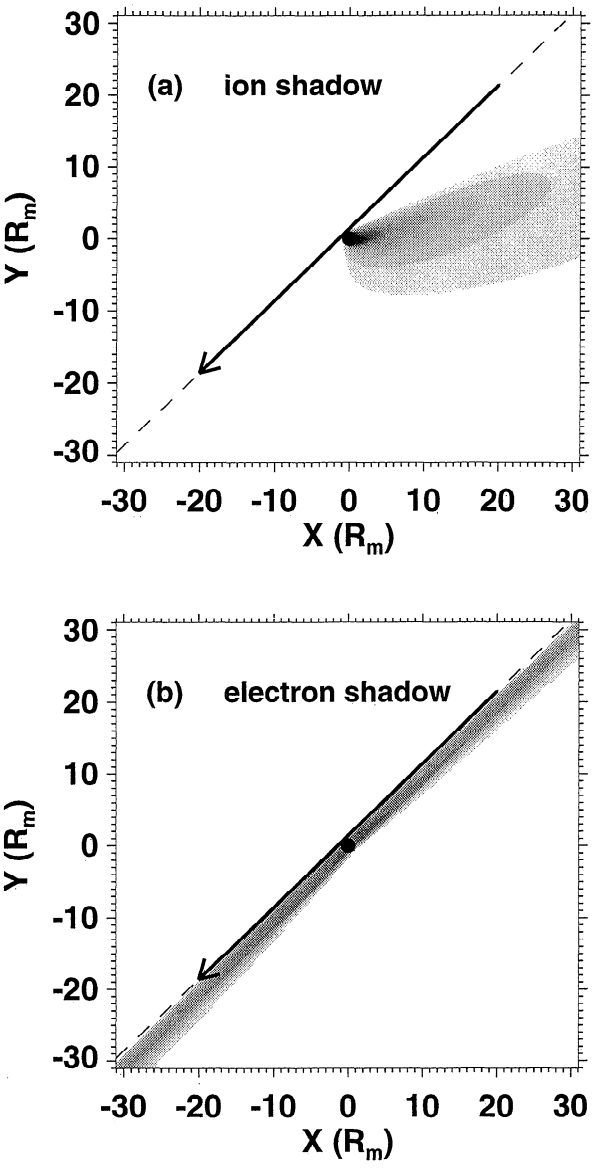

Figure 3. The (a) ion and (b) electron density shadows for $S_i = 1$ and $S_e = 1/43$. Although unrealistic in the solar wind, this figure shows how the density shadows would appear for $v_{sw} = v_{th}^p$. The ion density shadow is now receding back toward the tangent IMF lines, while the electron density shadow is almost perfectly field-aligned.

nearly contained within a cylinder of tangent field lines of one lunar radius and centered on the Moon. In Figure 4, the particle shadows are shown for $S_i = 30$ and $S_e = 30/43$, again unrealistic; here, the ion shadow is sharply constrained to the antisunward cylinder, while the electron shadow is now being forced back toward the antisunward region.

Since $S_s \propto \sqrt{m_s}$, the difference in shape of the lunar electron and ion density shadows is due primarily to the different particle masses. In the low-speed solar wind, the ratio of alpha to proton thermal speeds is often smaller than 1, and occasionally observed to be $v_{th}^{\alpha}/v_{th}^{p} = 1/2$. When these conditions obtain, there should be a slight difference in the shadowing properties of protons and alpha particles. Figure 5a shows the relative density profiles at a distance of $X = 7\ R_m$ antisunward of the Moon (similar to the Wind December 1994 encounter) with $v_{th}^{\alpha}/v_{th}^{p} = 1/2$; figure 5b shows n_α/n_p at the same distance. On the edge of the wake structure, the alpha/proton density ratio should be somewhat greater that its nominal solar wind value; in the middle of the wake, the ratio should be lower. Any deviation from this distribution must be due to ambipolar electric fields near the wake or edge effects near the Moon due to the different Larmor radii. This should be observable using the instrumentation on Wind; indeed, an effect on the distribution of alpha particles has been seen during the December 1994 encounter (J. T. Steinberg, personal communication, 1997) but has not yet been analyzed in detail. Figure 5c and 5d show the same profiles for a crossing point of $X = 20\ R_m$, which

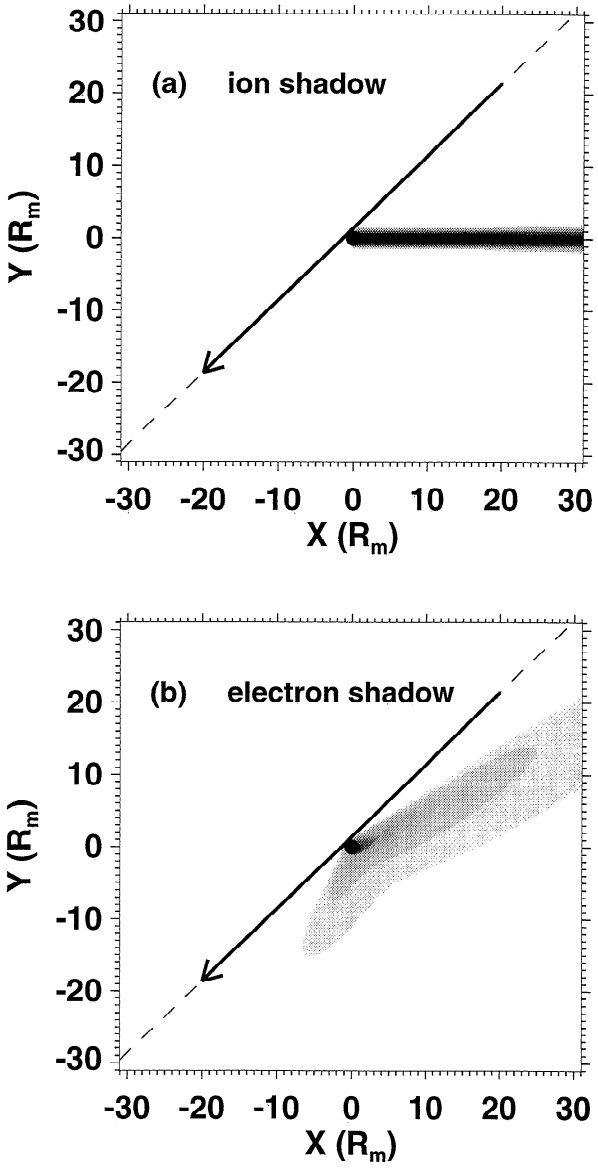

Figure 4. The (a) ion and (b) electron density shadows for $S_i = 30$ and $S_e = 30/43$. For very large S, the ion density shadow is almostly perfectly antisunward; the electron shadow is now being forced back toward the ion shadow by the large flow speed. This scenario is again unrealistic in the solar wind.

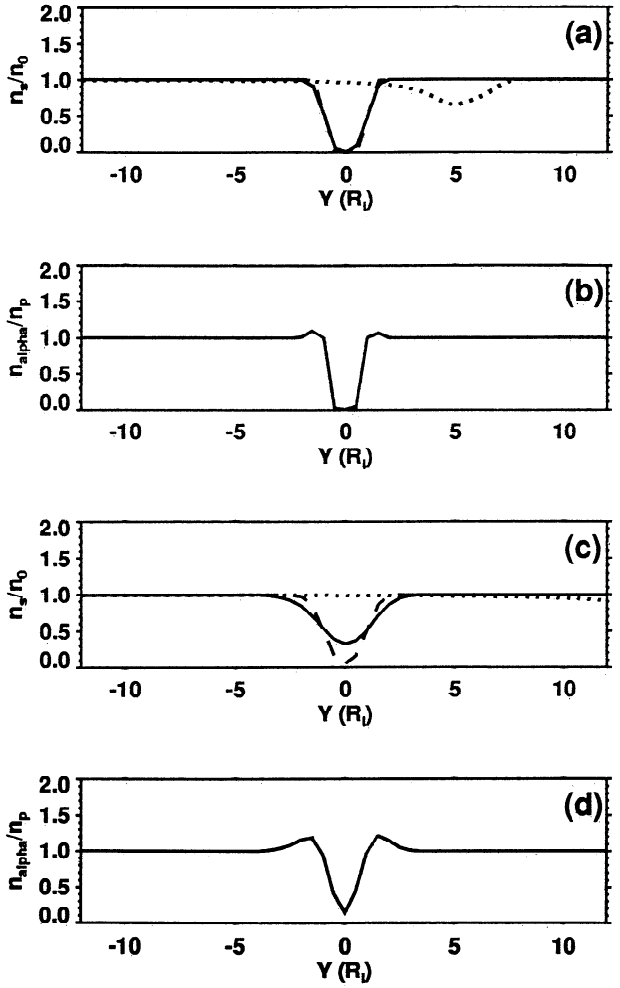

Figure 5. Relative density profiles through the wake. (a) n_{proton}/n_0 (solid line), $n_{electron}/n_0$ (dotted line), and n_{alpha}/n_0 (dashed line) antisunward of the Moon at X = 7 R_m; the electron shadow is deepest where the IMF crosses the plane. (b) The ratio of alpha to proton density (assuming $v_{th}^{\alpha}/v_{th}^{p} = 1/2$), relative to its ambient value. This model predicts a relative surplus of alpha particles just near the edge of the alpha/proton wake. (c) The various density profiles at $X = 20\ R_m$ and (d) the alpha to proton ratio. At this deeper distance, the variation in alpha to proton density may be easier to detect.

is relevant for other Wind lunar encounters. The electron density shadow is very shallow at this distance, but the effect on the relative alpha particle density may be easier to observe.

5. Discussion

There are two processes that fill a plasma wake near an uncharged body: (1) the thermal motion of the constituent particles and (2) the effect of space charge electric fields. The model outlined above describes only the first of these two processes. In reality, the deviations from neutrality will induce a potential (and hence a space charge field) through Poisson's equation. The space charge field will accelerate ions into the ion wake at roughly the ion acoustic speed; during this process, the electrons are considered Boltzmann ($n = n_0\ e^{e\phi/k_b T_e}$) and act to shield the ion density perturbations. Observations of counter-streaming ions in the wake [*Ogilvie et al.*, 1996] have prompted *Farrell et al.* [1997] to suggest that an ion-ion streaming instability generates ion acoustic noise in the region just antisunward of the Moon. This scenario is complementary to our model and seems likely given the ion currents needed to fill the ion density depletion region. Indeed, the formation of ion beams in the antisunward region has been observed in a simple electrostatic simulation (W. M. Farrell et al., A simple simulation of a plasma void: applications to Wind observations of the lunar wake, submitted to Journal of Geophysical Research, 1997, hereinafter referred to as submitted manuscript, 1997). In this same simulation, the electrons act to shield the ions in the antisunward wake.

Both particle instruments on the Wind spacecraft observed the ion wake to be just antisunward of the Moon [*Ogilvie et al.*, 1996; *Bosqued et al.*, 1996] as predicted by the model. Electron density measurements by the 3DP instrument [*Bosqued et al.*, 1996] show the deepest electron density depletion to be in the antisunward region as well, in agreement with the simulations (W. M. Farrell et al., submitted manuscript, 1997). Since the electrons are not shadowed heavily in this region (Figure 5a), this is evidence of the importance of space charge fields in restoring local quasineutrality.

In addition, *Bosqued et al.* [1996] show evidence of depleted electron density in the electron shadow region of Figure 2. At around 1700 UT of the December 1994 encounter, the spacecraft was magnetically connected to the wake near the Moon and within the electron shadow [*Bale et al.*, 1997]. At this time, the density of energetic electrons was somewhat decreased [*Bosqued et al.*, 1996], and intense Langmuir and ion acoustic waves were observed [*Bale et al.*, 1997]. In these regions of electron density depletion, some process must act on fast timescales in response to the space charge; in addition, the electron velocity distributions are inherently unstable to the generation of Langmuir waves. Since electron depletion regions are observed, the local distributions are not fully replenished and wave growth may be a steady state phenomenon. Therefore it seems that the lunar shadowing of solar wind electrons is important in understanding the interaction of the Moon with the solar wind. Extending the guiding center model of *Whang* [1968] to include solar wind electrons explains the plasma waves observations by Wind [*Kellogg et al.*, 1996; *Bale et al.*, 1996] and RAE-2 [*Weber et al.*, 1976] as well as Explorer 35 observations of electron density depletion guided by the IMF angle [*Lin*, 1968; *Van Allen and Ness*, 1969]. Solar wind ions are indeed depleted antisunward of the Moon, but the higher thermal speed of the electrons forces the electron density shadow away from the optical wake toward the magnetic field lines tangent to the Moon. The difference in the spatial ion and electron distributions is nonzero throughout much of the wake; hence space charge fields must exist throughout a large region of space on connected IMF lines. It is likely that the electron currents induced by the space charge fields would then generate the observed electrostatic ion acoustic waves. Langmuir waves will be generated by positive slope features in the shadowed electron distributions; this model is essentially the same as that of the terrestrial electron foreshock [*Filbert and Kellogg*, 1979]. The term forewake has been suggested [*Farrell et al.*, 1996]. Additionally, there may be an observable change in the alpha/proton ratio through the wake.

The presence of distinct regions of density depletion for ions and electrons underscores the kinetic nature of the Moon-solar wind interaction. Most theoretical work on plasma wakes has been done assuming particle ions and a Boltzmann distribution of electrons; while this does well to explain the ion wake behind the Moon, it is inadequate to explain the observation of electron density depletions and plasma waves with electron timescales. Our simple model shows that the electron density shadow should be controlled by the IMF direction, as observed by Explorer 35 and Wind experiments. A full particle simulation of the lunar wake would be a worthwhile and interesting undertaking.

Acknowledgments. SDB acknowledges discussions with C. J. Owen, W. M. Farrell and J. T. Steinberg and thanks G. Chisham for help with the figures. This work was supported in part by PPARC (UK) grants GR/L37748 and GR/L29347.

The editor thanks K. W. Ogilvie and J. M. Bosqued for their assistance in evaluating this paper.

References

Bale, S. D., C. J. Owen, J.-L. Bougeret, K. Goetz, P. J. Kellogg, R. P. Lepping, R. Manning and S. J. Monson, Evidence of currents and unstable particle distributions in an extended region around the lunar plasma wake, *Geophys. Res. Lett.*, *24*, 1427, 1997.

Bosqued, J. M., et al., Moon-solar wind interaction: First results from the Wind/3DP experiment, *Geophys. Res. Lett.*, *23*, 1259, 1996.

Cairns, I. H., The electron distribution function upstream from the Earth's bow shock, *J. Geophys. Res.*, *92*, 2315, 1987.

Farrell, W. M., R. J. Fitzenreiter, C. J. Owen, J. B. Byrnes, R. P. Lepping, K. W. Ogilvie, and F. Neubauer, Up-

stream ULF waves and energetic electrons associated with the lunar wake: Detection of precursor activity, *Geophys. Res. Lett.*, *23*, 1271, 1996.

Farrell, W. M., M. L. Kaiser, and J. T. Steinberg, Electrostatic instability in the central lunar wake: A process for replenishing the plasma void?, *Geophys. Res. Lett.*, *24*, 1135, 1997.

Filbert, P. C., and P. J. Kellogg, Electrostatic noise at the plasma frequency beyond the Earth's bow shock, *J. Geophys. Res.*, *84*, 1369, 1979.

Goldstein, B. E., Observations of electrons at the lunar surface, *J. Geophys. Res.*, *79*, 23, 1974.

Kellogg, P. J., K. Goetz, S. J. Monson, J.-L. Bougeret, R. Manning, and M. L. Kaiser, Observations of plasma waves during a traversal of the Moon's wake, *Geophys. Res. Lett.*, *23*, 1267, 1996.

Lin, R. P., Observations of lunar shadowing of energetic particles, *J. Geophys. Res.*, *73*, 3066, 1968.

Ogilvie, K. W., J. T. Steinberg, R. J. Fitzenreiter, C. J. Owen, A. J. Lazarus, W. M. Farrell, and R. B. Torbert, Observations of the lunar plasma wake from the Wind spacecraft on December 27, 1994, *Geophys. Res. Lett.*, *23*, 1255, 1996.

Owen, C. J., R. P. Lepping, K. W. Ogilvie, J. A. Slavin, W. M. Farrell, and J. B. Byrnes, The lunar wake at 6.8 R_l: Wind magnetic field observations, *Geophys. Res. Lett.*, *23*, 1263, 1996.

Schubert, G., and B. R. Lichtenstein, Observations of Moon-plasma interactions by orbital and surface experiments, *Rev. Geophys.*, *12*, 592, 1974.

Van Allen, J. A., and N. F. Ness, Particle shadowing by the Moon, *J. Geophys. Res.*, *74*, 71, 1969.

Weber, R. R., J. Fainberg, and R. G. Stone, Low frequency radio observations of the solar wind near the Moon, *Geophys. Res. Lett.*, *3*, 297, 1976.

Whang, Y. C., Interaction of the magnetized solar wind with the Moon, *Phys. Fluids*, *11*, 969, 1968.

Stuart D. Bale, Space Sciences Laboratory, University of California, Berkeley, CA 94720-7450 (email: bale@sunspot.ssl.berkeley.edu).

(Received March 25, 1997; revised June 4, 1997;
accepted June 4, 1997.)